

Research Article

Open Access



An improved artificial potential field method for multi-AGV path planning in ports

Xinqiang Chen^{1,2,3}, Chen Chen⁴, Huafeng Wu⁴, Octavian Postolache^{5,6}, Yuzhen Wu⁷

¹Institute of Logistics Science and Engineering, Shanghai Maritime University, Shanghai 201306, China.

²Chongqing Key Laboratory of Green Logistics Intelligent Technology, Chongqing Jiaotong University, Chongqing 400074, China.

³Jiangxi Key Laboratory of Intelligent Robot, Nanchang University, Nanchang 330000, Jiangxi, China.

⁴Merchant Marine College, Shanghai Maritime University, Shanghai 201306, China.

⁵Instituto de Telecomunicações (IT), North Tower, Lisbon 1049-001, Portugal.

⁶Department of Information Science and Technology, Iscte-Instituto Universitário de Lisboa, Lisbon 1649-026, Portugal.

⁷SPG Qingdao Port Group Co., Ltd. Shandong Port Group, CO.LTD., Qingdao 266011, Shandong, China.

Correspondence to: Yuzhen Wu, SPG Qingdao Port Group Co., Ltd. Shandong Port Group, CO.LTD., No. 7 Gangji Road, Qingdao 266011, Shandong, China. E-mail: wuyz@qdport.com

How to cite this article: Chen, X.; Chen, C.; Wu, H.; Postolache, O.; Wu, Y. An improved artificial potential field method for multi-AGV path planning in ports. *Intell. Robot.* **2025**, *5*, 19-33. <https://dx.doi.org/10.20517/ir.2025.02>

Received: 22 Sep 2024 **First Decision:** 15 Nov 2024 **Revised:** 15 Dec 2024 **Accepted:** 17 Dec 2024 **Published:** 11 Jan 2025

Academic Editors: Simon Yang, Yueying Wang **Copy Editor:** Pei-Yun Wang **Production Editor:** Pei-Yun Wang

Abstract

As global maritime transport rapidly advances, the demands for intelligent, safe, and efficient automated container ports have significantly increased. In this evolving landscape, multi-automated guided vehicle (AGV) systems have emerged as a critical element of port automation, playing an essential role. Within automated container terminals, quay cranes, AGVs, and yard cranes are the primary equipment for loading and unloading operations on ships. However, the complexity of simultaneously considering numerous practical factors and the intricate relationships among them has made optimization modeling in this area a challenging task. To tackle this challenge, we have developed a path optimization model for multi-AGV systems in port environments, based on an enhanced artificial potential field (APF) algorithm. This algorithm utilizes the initial states of AGVs, target locations, and obstacle information as inputs. It creates attractive forces near the target locations and repulsive forces around static obstacles. Moreover, a minimum safety distance between AGVs is established; when AGVs approach closer than this threshold, the algorithm introduces repulsive forces between them to prevent collisions. The algorithm dynamically recalculates the repulsive potential field in response to real-time feedback and changes in the environment, enabling continuous adjustment to the AGV paths and action plans. This iterative process continues until all AGVs reach their designated targets. The effectiveness of this algorithm has been validated through port



© The Author(s) 2025. **Open Access** This article is licensed under a Creative Commons Attribution 4.0 International License (<https://creativecommons.org/licenses/by/4.0/>), which permits unrestricted use, sharing, adaptation, distribution and reproduction in any medium or format, for any purpose, even commercially, as long as you give appropriate credit to the original author(s) and the source, provide a link to the Creative Commons license, and indicate if changes were made.



www.oaepublish.com/ir

environment simulations, demonstrating clear advantages in enhancing the safety and smoothness of multi-AGV path planning.

Keywords: Automated guided vehicles (AGVs), path planning, improved APF algorithm, autonomous port

1. INTRODUCTION

Ports, as critical hubs for international trade, not only undertake the centralized distribution, loading and unloading, and transportation of goods, but also play a vital role in the global supply chain. As global trade volume continues to grow, the transportation demand of ports is climbing annually, placing a higher emphasis on the efficiency, reliability and safety of port logistics^[1]. In this context, automated guided vehicles (AGVs), with their high efficiency, flexibility and intelligence, are gradually replacing the traditional equipment for transferring, loading, unloading and handling goods, dramatically reducing errors and delays brought about by manual operation, and have become an indispensable and important part of the port logistics system^[2]. Port operating environment is more complex, characterized by spatial complexity, high-density transportation tasks and various dynamic factors (e.g., the movement of ships, machinery and equipment), placing higher demands on AGV path planning; at the same time, as a key link connecting the shore bridge and the yard, the AGV plays an important role in improving the operational efficiency and overall operational performance of the port. The multi-AGV path planning problem can be described as follows: in a specific map environment, plan the optimal or near-optimal traveling path for each AGV from the starting point to the endpoint without collision and in compliance with the constraint rules, where the optimal objective can be the shortest traveling distance, the least traveling time, the least energy loss, etc. The optimal objective can be the shortest traveling distance, the least traveling time, the least energy loss, etc. In this paper, we propose a new approach to the multi-AGV path planning problem^[3]. The quality of path planning directly affects the efficiency of AGVs and the operational efficiency, safety and economic benefits of the port.

By leveraging data from a combination of sensors such as light detection and ranging (LiDAR) sensors, cameras, and global positioning systems (GPS), AGVs can perceive their surroundings in real time, enabling efficient path planning and obstacle avoidance in both complex and dynamic environments^[4]. This real-time sensing capability is essential for precise single-AGV path planning and serves as a strong foundation for multi-AGV path planning systems. Building on this, recent research has further refined single-AGV path planning algorithms, transitioning from classic approaches such as the Dijkstra algorithm^[5] and A* algorithm^[6] to more advanced techniques such as the artificial potential field (APF) algorithm^[7]. These developments have improved critical aspects such as obstacle avoidance, path optimization, and adaptability to dynamic conditions. For instance, Tang *et al.* proposed a geometric A* algorithm that utilizes a grid-based model to represent the port environment. By applying the functions $P(x, y)$ and $W(x, y)$, the algorithm filters out unsuitable nodes, thereby avoiding irregular paths. To enhance the smoothness and stability of AGV turning trajectories, cubic B-spline curves are employed to replace traditional polyline paths^[8]. Yin *et al.* developed a path-planning algorithm that integrates a kinematic-constrained A* algorithm with the dynamic window approach (DWA). In this method, the A* algorithm handles global path planning, while DWA manages dynamic local path adjustments. By optimizing nodes, refining the heuristic function, and introducing a secondary redundancy strategy, the algorithm reduces the number of sub-nodes and redundant nodes. The use of cubic B-spline curves further refines the path, moving it closer to the global optimal solution^[9]. Meng *et al.* present a lane-change trajectory prediction model based on a multi-task deep learning framework. It independently models trajectory changes in both directions during the lane-change process and facilitates information interaction and fusion through the multi-task learning approach, with the goal of improving safety^[10]. Wu *et al.* introduced a Bi-directional rapidly exploring

random tree (Bi-RRT)-based algorithm, specifically designed for navigating narrow passages, called narrow channel Bi-RRT (NCB-RRT). This approach introduces the research failure rate threshold (RFRT) and employs a three-stage search strategy to guide the generation of sampling points. Additionally, parent node reselection and path pruning are applied to reduce redundant nodes and shorten the overall path. The final trajectory is further smoothed using piecewise quadratic Bézier curves, resulting in improved path smoothness^[11].

In intelligent ports and large-scale operations, as the number of AGVs grows, problems such as waiting, conflicts, and deadlocks frequently arise, increasing the complexity of multi-AGV path planning. Traditional single-AGV path planning techniques are no longer adequate to meet these demands. To address these challenges, more advanced coordination and optimization mechanisms are needed for scheduling and resource management in multi-AGV systems. Researchers have been actively exploring improved path-planning algorithms to boost the efficiency of AGV systems. The A* algorithm, a classic pathfinding method, serves as the foundation for many enhanced versions. Li *et al.* introduced a path planning and navigation approach for robots, leveraging an enhanced A* algorithm alongside the DWA. Using laser radar, a map of densely planted jujube orchards was created, while the robot's position was identified through adaptive Monte Carlo localization. The method integrates both global and real-time local path planning, with the route further refined by an evaluation function for optimal navigation^[12]. Cui *et al.* introduced a path-planning approach that integrates the hybrid A* algorithm with geometric curves. Initially, the hybrid A* algorithm performs global path planning, ensuring the route from the parking entrance to the designated space is viable. Following this, genetic algorithms are employed for local optimization, improving both the safety and efficiency of the path^[13]. Sun *et al.* addressed the shortcomings of particle swarm optimization (PSO) in high-dimensional environments by proposing an improved multi-objective PSO (IMOPSO), enhancing global search capabilities with adaptive differential evolution strategies and iterative local search^[14]. Huang *et al.* introduced a density gradient-RRT algorithm, an extension of the RRT algorithm, utilizing a dynamic gradient sampling strategy to enhance the initial solution's efficiency and reconstruct the path to reduce overall costs^[15]. Wang *et al.* developed an improved bidirectional obstacle-edge search artificial potential field RRT* algorithm (IBPF-RRT*), optimizing branching nodes and using a triangle inequality pruning strategy to enhance path quality and reduce iteration times for convergence^[16]. Xu *et al.* introduced a two-stage scheduling-based optimal path planning method for multi-AGV systems. In the offline phase, they employed a high-performance genetic algorithm for path planning in a static environment, addressing challenges such as premature convergence and obstacle avoidance. During the online phase, the system identifies various types of conflicts between AGVs, including node, opposing, and chasing conflicts, and resolves them to ensure real-time collision-free scheduling^[17]. Huang *et al.* introduce a Copula-based joint model to analyze the simultaneous destination and route choice behaviors during the search process^[18]. Zhou *et al.* presented a path-planning approach based on an improved conflict-based search (ICBS) algorithm, constructing detailed models of the environment, tasks, objectives, and constraints. The method follows a two-tier structure, where the lower tier uses an enhanced A* algorithm to optimize node selection, while the upper tier manages conflicts by assigning conflict numbers, targets, and a conflict constraint set. The algorithm also introduces three conflict prioritization rules - most conflicts first (MCF), earliest conflict first (ECF), and single search of conflict points (SSCP) - along with strategies for conflict resolution^[19]. Wu *et al.* enhanced the APF method by incorporating gain constraints and stochastic factors, employing B-spline curve optimization to smooth paths, reducing oscillations, and mitigating local minima issues^[20]. Nazarabari *et al.* proposed a path-planning method using an enhanced genetic algorithm (EGA), finding feasible initial paths with time-efficient deterministic strategies and optimizing them through custom crossover and mutation operators^[21]. Ning *et al.* developed a hybrid multi-strategy rapid exploration random tree (HMS-RRT) method for multi-robot cooperative exploration, improving exploration efficiency and robustness in unknown environments through adaptive

incremental distance, Voronoi diagram partitioning, and optimized task allocation^[22]. Liu *et al.* propose a two-layer stacked framework to analyze time and distance gaps, enabling more accurate decision-making^[23]. Mai *et al.* introduced a dual-strategy ant colony algorithm. By improving the state transition probability rule and introducing a deterministic selection strategy, they redefined the movement rules of ants. Heuristic information such as neighboring node distance and elevation is added to enhance search efficiency. Additionally, a dynamic pheromone update strategy is proposed to optimize global search and convergence, preventing local optima. The result is a new Ant Colony Optimization (ACO) variant, called the dual-strategy ACO algorithm^[24]. These advanced multi-AGV path planning algorithms not only improve single-AGV path planning but also offer effective solutions for the coordination and optimization of multi-AGV systems, advancing intelligent logistics and automation systems in ports and beyond.

In the realm of modern industrial automation and intelligent transport systems, AGVs have emerged as vital tools for boosting production efficiency and cutting labor costs. Traditional path planning algorithms are celebrated for their dependability and performance, while the APF method, through its use of potential fields, excels at obstacle avoidance and adaptability in dynamic settings. However, conventional APF is primarily geared toward single-AGV path planning, relying predominantly on distance-based fields to guide navigation. Although this method works well for single-AGV obstacle avoidance, it struggles to optimize performance in complex multi-AGV collaborative environments, failing to meet the demands for high efficiency and safety in real-world applications. Our research goes beyond simply applying the APF method, offering substantial improvements by introducing a multi-AGV collision avoidance mechanism. These enhancements significantly bolster the APF algorithm's effectiveness in multi-AGV systems operating in complex and dynamic environments.

The key contributions are as follows:

- (1) By segmenting the attraction function and optimizing the repulsion function, the robustness of path planning can be significantly improved.
- (2) Incorporating a potential field interaction function between AGVs within the APF framework enhances collision avoidance and ensures system-wide stability and safety during multi-AGV coordination.
- (3) Expanding the traditional APF algorithm to extend its application from single-AGV path planning to multi-AGV collaborative and independent path planning enhances its adaptability and efficiency in complex dynamic environments.

2. THE PROPOSED METHOD

The APF algorithm, initially introduced by Khatib^[25], is inspired by the principle of electromagnetic field in science, and establishes an APF within a virtual environment. In the virtual potential field, there are both gravitational and repulsive fields; the repulsive potential field will be generated around the obstacles and the impassable area, and the gravitational potential field will be generated around the target point. Additionally, by synthesizing the effect of these forces, the movement can be along the gradient direction of the potential field, so as to realize the path planning.

2.1. Attraction and repulsion model

In a multi-AGV system, each AGV is equally driven by the potential field forces, and thus an APF algorithm is required to perform independent path planning for each AGV. In this situation, the APF algorithm needs to dynamically adjust the potential field forces according to the current state of each AGV, including speed,

direction, and position, as well as the obstacles present in the environment.

The state information of each AGV is utilized by the APF algorithm to define its environment within the simulated potential field model and is driven by the potential field force. The attractive potential energy that an AGV experiences is directly related to its distance from the target point; the farther the AGV is from the target, the higher the potential energy it detects. As the AGV approaches the target, this potential energy diminishes. Consequently, the closer the AGV gets to the target, the weaker the attractive force becomes, guiding the AGV smoothly to its destination. The distance between each AGV and the target point can be determined by the Euclidean distance formula, which is the core parameter of the attractive potential field, as given in

$$\|q - q_g\| = \sqrt{(x_1 - x_2)^2 + (y_1 - y_2)^2} \quad (1)$$

The attractive potential field function based on the distance is defined by

$$Ua(q) = \begin{cases} \frac{1}{2} \varepsilon [\rho(q, q_g)]^2; 0 \leq \|q - q_g\| \leq d_g \\ \varepsilon d_g \rho(q, q_g) - \frac{1}{2} \varepsilon d_g^2; \|q - q_g\| > d_g \end{cases} \quad (2)$$

By taking the negative gradient of this function, the magnitude and direction of the attractive force acting on the AGV can be derived, as given in

$$Fa(q) = -\nabla Ua(q) \quad (3)$$

$$Fa(q) = \begin{cases} \varepsilon \rho(q, q_g); 0 \leq \|q - q_g\| \leq d_g \\ \varepsilon d_g \frac{\rho(q, q_g)}{\|q - q_g\|}; \|q - q_g\| > d_g \end{cases} \quad (4)$$

Where $\|q - q_g\|$ represents the distance between two coordinate points, (x_1, y_1) denotes the coordinates of the current position of the AGV, while (x_2, y_2) indicates the coordinates of the target point. ε is the scale factor and d_g is the range of influence of the attraction. $\rho(q, q_g)$ denotes the vector distance between the current position q of the AGV and the target point position q_g , which is oriented in the direction of the AGV position pointing to the target point position.

When the AGV is at a distance $\rho(q, q_g) \leq d_g$ from the target point, the attractive force is linearly related to the distance. When the AGV is at a distance $\rho(q, q_g) > d_g$ from the target point, the magnitude of the attraction tends to be saturated with respect to the direction of the target point.

Compared with the traditional APF algorithm, this formula uses a piecewise function to dynamically adjust the magnitude of the attractive force instead of relying on a fixed value. This approach ensures that the AGV is consistently guided by the attractive force throughout the path-planning process while adapting its trajectory based on the distance to the target point. By moderating the attractive force when the AGV is farther from the target, the algorithm prevents excessive velocity increases, resulting in smoother movement and minimizing abrupt path changes.

The repulsive potential energy of each AGV is inversely proportional to its distance from static obstacles, measured from the surface of the obstacle to the AGV. As the distance between the AGV and the obstacle increases, the repulsive potential energy experienced by the AGV decreases. Conversely, as the obstacle moves closer to the AGV, the repulsive potential energy increases accordingly. This potential field function is given in

$$Ur_{obs}(q) = \begin{cases} \frac{1}{2} Kr \left(\frac{1}{[\rho(q, q_0)]^2} - \frac{1}{\rho_0^2} \right)^2; & 0 \leq \|q - q_0\| \leq \rho_0 \\ 0; & \|q - q_0\| > \rho_0 \end{cases} \quad (5)$$

and its resulting repulsive force is expressed as

$$Fr_{obs}(q) = \begin{cases} Kr \left(\frac{1}{[\rho(q, q_0)]^2} - \frac{1}{\rho_0^2} \right) \frac{2}{[\rho(q, q_0)]^3} \frac{\rho(q, q_0)}{\|q - q_0\|}; & 0 \leq \|q - q_0\| \leq \rho_0 \\ 0; & \|q - q_0\| > \rho_0 \end{cases} \quad (6)$$

where K_r is the repulsive potential field gain factor. ρ_0 is a constant that represents the upper limit distance at which the obstacle affects the AGV. $\rho(q, q_0)$ represents the distance $\|q - q_0\|$ between the current position q of the AGV and the closest point q_0 of the obstacle area around the AGV, which points to the direction from the obstacle to the AGV. Traditional APF methods calculate the repulsive force by evaluating the gradient of the distance. In contrast, this implementation computes the repulsive force directly from the vector connecting the AGV's current position to the center of the obstacle. This method streamlines the calculations and more accurately represents the real-world repulsive effects encountered in practical situations.

2.2. Collision avoidance between multiple AGVs

Traditional APF algorithms are primarily designed for path planning of individual AGVs, focusing on helping the AGV navigate around static obstacles. However, in a multi-AGV system, each AGV must not only avoid static obstacles in the environment but also address collision avoidance with other AGVs. Conversely, other AGVs are regarded as dynamic obstacles within the simulation. The relative motion between AGVs greatly heightens the risk of trajectory conflicts. Therefore, additional considerations must be incorporated into the path-planning process to ensure that collisions between AGVs are avoided.

To ensure the safe operation of multi-AGV systems, the algorithm incorporates a predefined safety distance threshold. When the actual distance between two or more AGVs falls below this threshold, the system applies a repulsive force to push them apart, effectively preventing collisions. The safety distance threshold is carefully designed by considering various factors, such as the operating speed, braking capabilities, and dynamic environmental conditions of AGVs, to balance safety requirements with operational efficiency.

The intensity of the repulsive force is inversely proportional to the distance between AGVs: the closer they are, the stronger the repulsive force, prompting AGVs to quickly take evasive actions. Conversely, as the distance increases and exceeds the safety threshold, the repulsive force gradually weakens and eventually disappears, avoiding unnecessary interference with the normal path planning of AGVs. To enhance the precision of evasive maneuvers, the system dynamically monitors real-time AGV status, including position, speed, and direction. Based on this data, the algorithm adjusts the magnitude and direction of the repulsive force, ensuring the reasonableness of the avoidance path. The repulsive potential energy between AGVs is defined by

$$Ur_{\text{agv}}(q) = \begin{cases} \frac{1}{2}\delta\left(\frac{1}{\rho(q, q_{\text{other-agv}})} - \frac{1}{d}\right)^2; & 0 \leq \|q - q_{\text{other-agv}}\| \leq d \\ 0; & \|q - q_{\text{other-agv}}\| > d \end{cases} \quad (7)$$

Then, the function of repulsive force between AGVs is given in

$$Fr_{\text{agv}}(q) = \begin{cases} \delta\left(\frac{1}{\rho(q, q_{\text{other-agv}})} - \frac{1}{d}\right)\frac{1}{\left[\rho(q, q_{\text{other-agv}})\right]^2} \frac{\rho(q, q_{\text{other-agv}})}{\|q - q_{\text{other-agv}}\|}; & 0 \leq \|q - q_{\text{other-agv}}\| \leq d \\ 0; & \|q - q_{\text{other-agv}}\| > d \end{cases} \quad (8)$$

Where δ is the repulsion coefficient, which controls the strength of the repulsive force; d is the safe distance between AGVs, i.e., the minimum allowable distance; and $q_{\text{other-agv}}$ denotes the coordinates of an AGV that may conflict with the current AGV, respectively. $\rho(q, q_{\text{other-agv}})$ indicates the distance $\|q - q_{\text{other-agv}}\|$ between the two agvs, whose direction points from $q_{\text{other-agv}}$ to q .

2.3. Combined force formula

The total potential energy of the current AGV is calculated by

$$U_{\text{total}}(q) = Ua(q) + Ur_{\text{obs}}(q) + Ur_{\text{agv}}(q) \quad (9)$$

The total potential field force, which results from the combined effects of all attractive and repulsive forces, is defined by

$$F_{\text{total}}(q) = Fa(q) + Fr_{\text{obs}}(q) + Fr_{\text{agv}}(q) \quad (10)$$

The magnitude and direction of this force play a crucial role in determining the next movement state of the AGV. Specifically, the force's direction guides the AGV toward the target point while simultaneously steering it away from obstacles, ensuring adaptability and stability during the path-planning process.

However, in complex potential field environments, the AGV may encounter situations where the attractive and repulsive forces reach equilibrium, causing it to get trapped in a local minimum and halting its movement. To address this issue, the system incorporates a random perturbation mechanism. When the AGV's position change approaches zero, a small random force is applied to help it escape the local minimum. The amplitude of this random perturbation is carefully designed to provide sufficient disturbance for the AGV to overcome local minima while maintaining the overall smoothness and stability of the planned path.

The flowchart of the improved APF algorithm is shown in [Figure 1](#).

3. EXPERIMENTATION

3.1. Port environment simulation

Ports can be classified into vertical, parallel, and U-shaped terminal layouts based on the arrangement of their facilities. In a parallel terminal layout, key elements such as quay cranes, containers, AGVs, and the container yard are aligned in parallel rows. Conversely, in a vertical terminal layout, these facilities are arranged perpendicularly to the quay. The U-shaped terminal layout features a unique configuration, where the container yard is designed in a U-shape, facilitating simultaneous loading and unloading of containers.

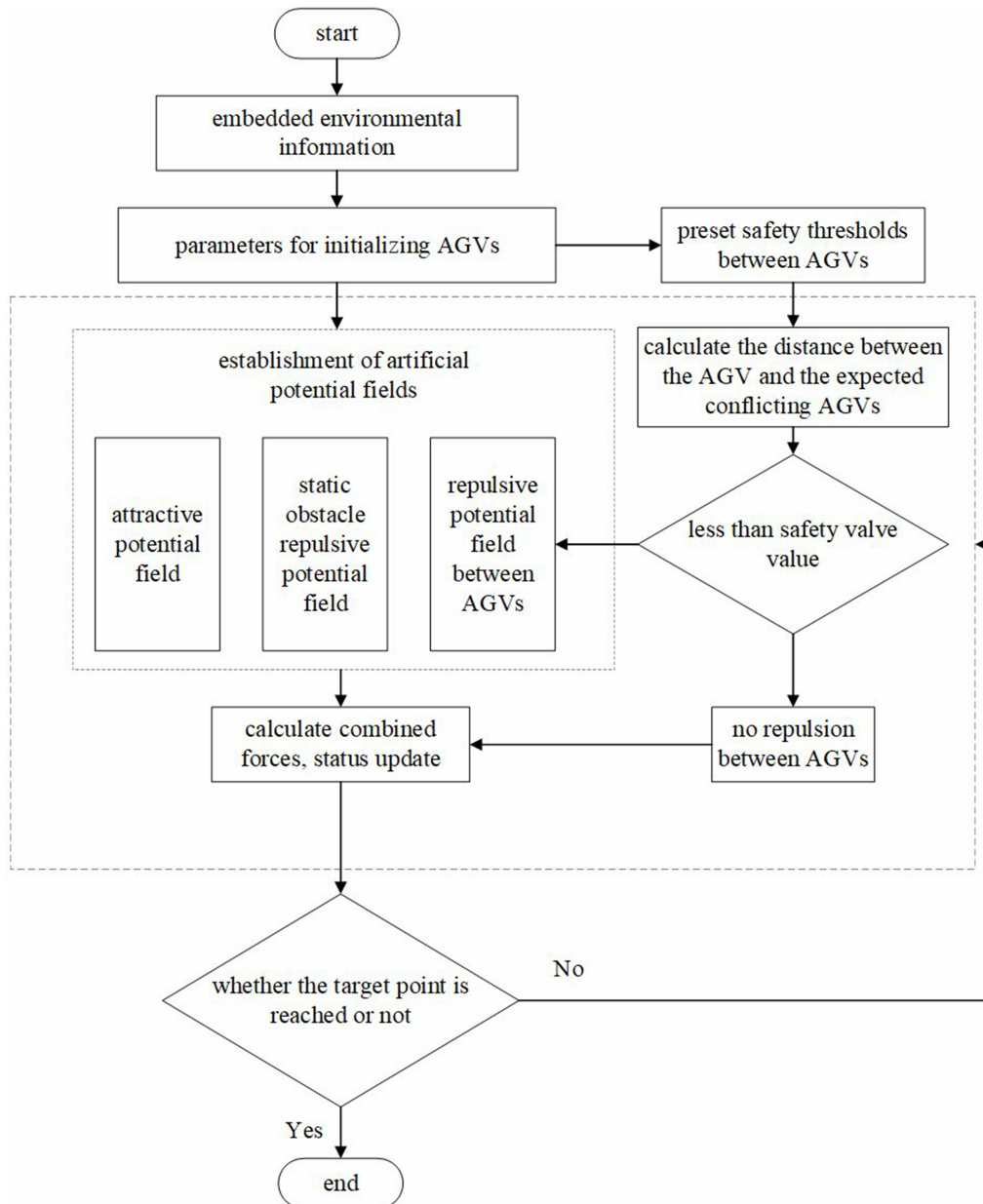


Figure 1. Flowchart of the improved APF algorithm. APF: Artificial potential field.

In real-world port environments, the layout selection is primarily influenced by factors such as available space, cargo throughput, and the port's operational strategy. For large container ports, the parallel layout is ideal for high throughput as it facilitates more simultaneous operations. In contrast, the vertical layout is better suited for ports with limited space or requiring rapid cargo transfers. The U-shaped layout is typically used in ports with specialized functions or where space is constrained but efficient loading and unloading operations are essential.

As depicted in [Figure 2](#), the simulation of the port environment is based on these vertical and parallel layouts to accurately reflect the real-world arrangement of key facilities and the operating environment for a multi-AGV system. The model incorporates essential facilities such as quay cranes, storage yards, and

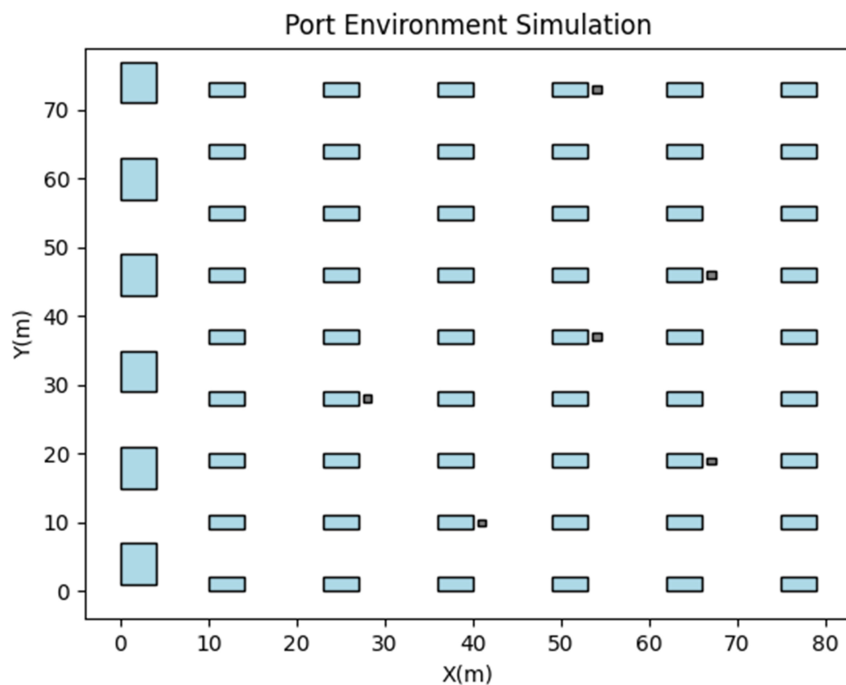


Figure 2. Simulated port environment.

container storage points, which are considered static obstacles during multi-AGV path planning, while other AGVs are treated as dynamic obstacles. Quay cranes and yard facilities are depicted as light blue rectangular cells in the simulation, with six quay cranes and 54-yard cells included to replicate their actual size and positioning within the port. Containers and storage points are represented by gray square cells to distinguish container storage areas. Each cell corresponds to a length of 1 meter, ensuring that the spatial scale in the simulation closely mirrors the real environment.

3.2. Experimental settings

In the simulated port environment, the setup includes 54 fixed obstacles and six AGVs, with their dimensions and positions predefined in the simulation code. Each AGV begins at a specific starting location and aims to reach a designated endpoint. An AGV can handle only one task at a time and is not permitted to return to the starting point until the current task is complete. The primary challenge for each AGV is to navigate through a complex environment to find the most efficient path to its destination, ensuring safety while minimizing travel time. The simulation focuses on the task of unloading containers, so all AGVs are operating without loads as they move from the container yard to the quay crane.

As AGVs move within the port environment, the algorithm continuously monitors the position and direction of each AGV in real-time, dynamically adjusting their path planning based on comparisons with the current information of other AGVs to address potential conflicts or bottlenecks. When the distance between any AGV and others falls below a predefined conflict threshold, the algorithm identifies these AGVs as having a potential conflict. Upon detecting a potential conflict, the algorithm initiates a conflict resolution mechanism.

3.3. Experimental results

Each of the six AGVs was assigned a task based on the port layout described. The starting and ending coordinates for these transportation tasks are listed in [Table 1](#). Each AGV conducts its task of moving

Table 1. AGVs, start and end points, and color settings

AGVs numbering	Starting point	Endpoint	Color
AGV1	(5, 4)	(67, 19)	Blue
AGV2	(5, 18)	(54, 37)	Orange
AGV3	(5, 32)	(41, 10)	Green
AGV4	(5, 46)	(54, 73)	Red
AGV5	(5, 60)	(67, 46)	Purple
AGV6	(5, 74)	(18, 28)	Brown

AGVs: Automated guided vehicles.

containers from the quay crane to the container yard, with each one designated by a specific color and label, ensuring an organized port operation. The AGVs are sequentially labeled from AGV1 to AGV6 and are distinguished by the blue, orange, green, red, purple, and brown colors. This color-coded system facilitates easy identification and tracking of movements of each AGV across the port. By continuously monitoring the operational status of AGVs, the algorithm can swiftly detect potential path conflicts or delays and implement necessary adjustments.

In this comparative experiment, the improved APF algorithm is evaluated against the traditional APF algorithm, the A* algorithm, and the probabilistic roadmap algorithm (PRM) algorithm. **Table 2** provides a detailed overview of the parameter configurations for both algorithms used in the study.

Figure 3 illustrates the trajectory maps generated by four algorithms for six transportation tasks: the improved APF algorithm (A), the traditional APF algorithm (B), the A* algorithm (C), and the PRM algorithm (D). In these trajectory maps, the start and goal positions of each AGV are marked with colored circles. The circles near the quay cranes indicate the starting positions, while those near the container yard represent the designated goal positions. Black circles along the paths denote intersections or turning points.

All AGVs start simultaneously from their designated initial positions, traveling at the same speed to ensure a more intuitive and fair comparison of the path-planning performance of the four algorithms. As shown in **Figure 3A**, the paths of AGV5 and AGV6 have intersections but no conflicts occur. This is primarily because the starting positions of the AGVs are sufficiently far apart, resulting in differences in both the paths taken and the times they reach the intersection points, effectively avoiding potential collisions. Furthermore, **Figure 3A** highlights a completely independent path with no intersections, specifically the path planned for AGV1. This unique characteristic is absent in the results of other algorithms, demonstrating the ability of the improved APF algorithm to minimize path intersections and enhance path independence. In contrast, **Figure 3B**, representing the traditional APF algorithm, reveals a higher number of intersections and overlapping paths, indicating its limitations in avoiding path conflicts. In **Figure 3C**, the A* algorithm exhibits significant path overlaps in the area between the container yard and the yard cranes, which not only reduces transportation efficiency but also increases the risk of congestion and collisions during AGV operation. Meanwhile, **Figure 3D** shows the results of the PRM algorithm, where the paths are more irregular and contain numerous sharp turns compared to the improved APF algorithm. This lack of smoothness in path planning may negatively affect AGV motion stability and energy efficiency. In terms of path smoothness, the improved APF algorithm in **Figure 3A** outperforms the other three algorithms, as their paths exhibit noticeable sharp turns. Such abrupt changes in direction can limit AGV travel speed, increase travel time and energy consumption, and exacerbate these issues in complex port environments. Additionally, sharp turns may impose greater stress on AGV hardware, leading to increased wear and tear and potentially shortening the lifespan of equipment.

Table 2. Algorithm parameter configuration

Parameter name	Numerical value
Attractive potential field scale factor	0.5
Repulsive potential field scale factor	1.0
Area of influence of the target point	3.0 m
Minimum safe distance between AGVs	2.0 m
Safety margin between AGVs and obstacles	3.0 m
Pacemaker	1.0 m/s
Obstacles size	2.0 m × 1.0 m
AGVs dimensions	1.0 m × 1.0 m

AGVs: Automated guided vehicles.

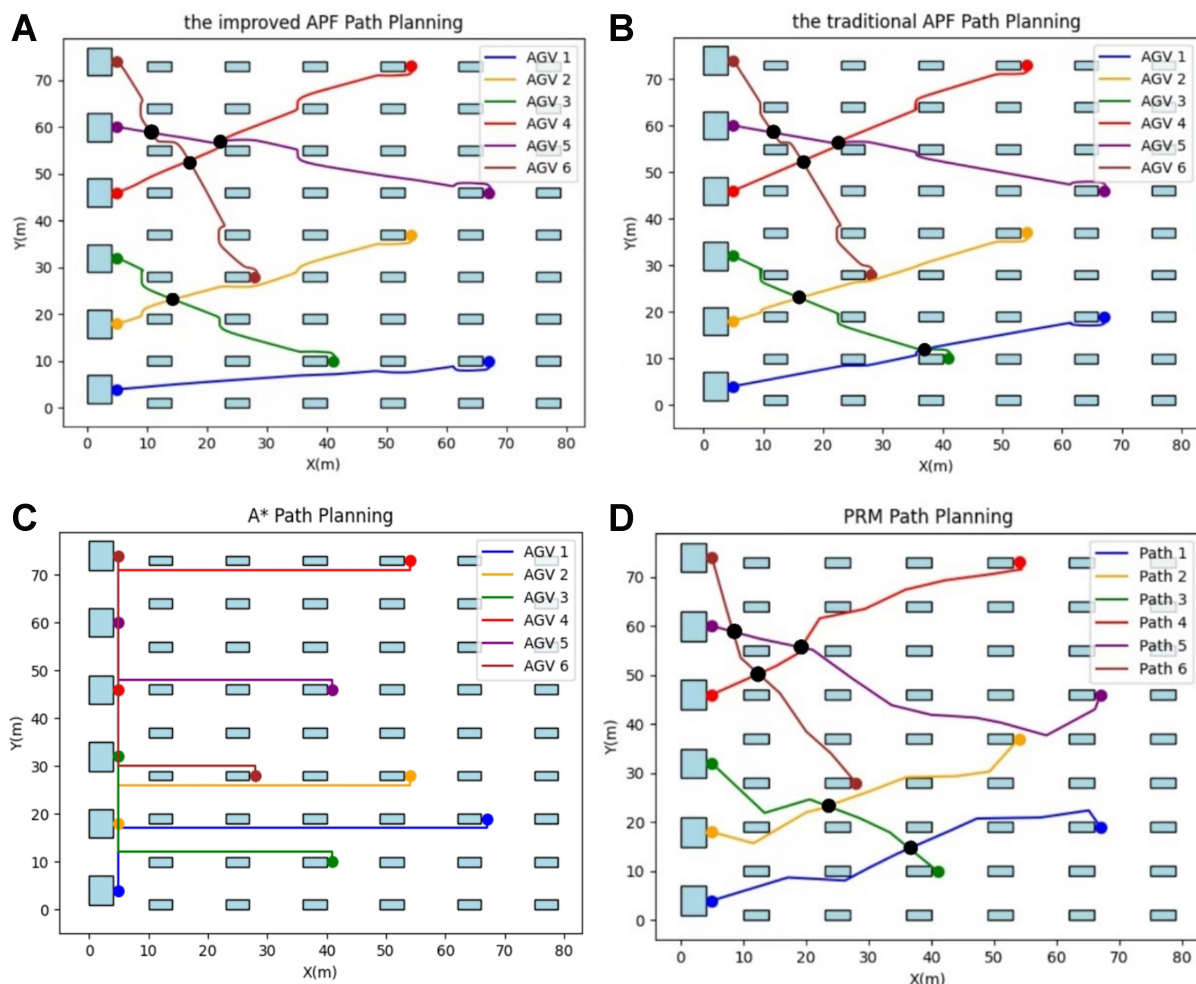


Figure 3. Path effect diagrams for the four algorithms. (A) the improved APF algorithm; (B) the traditional APF algorithm; (C) A* algorithm; (D) PRM algorithm. APF: Artificial potential field; PRM: probabilistic roadmap algorithm.

The experimental data in [Tables 3](#) and [4](#) highlight the improved APF algorithm as the most effective among the four methods, excelling in path length, planning time, and intersection point reduction. It achieves the shortest total path length (327.97 m), the fastest planning time (1.30 s), and the fewest intersection points (4), showcasing exceptional efficiency and conflict resolution in multi-AGV systems. The traditional APF

Table 3. Comparison of experimental data for different algorithms

AGVs numbering	Algorithms	Length (m)	Time spent on route planning (s)	Number of intersection points
AGV1	The improved APF	62.29	0.22	0
	The traditional APF	63.79	0.25	1
	A*	77.00	0.26	-
	PRM	68.01	11.30	1
AGV2	The improved APF	52.55	0.21	1
	The traditional APF	52.73	0.23	1
	A*	60.00	0.99	-
	PRM	56.91	11.17	1
AGV3	The improved APF	42.19	0.22	1
	The traditional APF	42.52	0.22	1
	A*	59.00	0.20	-
	PRM	44.59	11.14	2
AGV4	The improved APF	55.95	0.21	2
	The traditional APF	55.90	0.21	2
	A*	77.00	0.32	-
	PRM	60.08	11.02	2
AGV5	The improved APF	63.56	0.22	2
	The traditional APF	63.60	0.21	2
	A*	51.00	0.12	-
	PRM	71.43	11.25	2
AGV6	The improved APF	51.43	0.22	2
	The traditional APF	51.45	0.20	2
	A*	70.00	0.22	-
	PRM	55.10	11.30	2

AGVs: Automated guided vehicles; APF: artificial potential field; PRM: probabilistic roadmap algorithm.

Table 4. Summary of experimental data

Algorithms	Total length (m)	Total time spent on route planning (s)	Total number of intersection points
The improved APF	327.97	1.30	4
The traditional APF	329.99	1.31	5
A*	395.00	2.11	-
PRM	356.12	67.18	5

APF: Artificial potential field; PRM: probabilistic roadmap algorithm.

algorithm delivers reasonable performance, with a slightly longer path (329.99 m) and one additional intersection point, while maintaining comparable planning speed. In contrast, the A* algorithm produces significantly longer paths (395.00 m) and demonstrates limited effectiveness in minimizing conflicts. The PRM algorithm, while highly adaptable, is hindered by its excessive planning time (67.18 s) and the highest number of intersection points (5), making it less suitable for real-time applications.

From the comparison of the four path planning algorithms depicted, the improved APF algorithm stands out for its excellent path smoothness, effective obstacle avoidance, and strong coordination among multiple AGVs. It successfully overcomes the shortcomings of the traditional APF algorithm, which often encounters issues such as oscillations and local minima in complex environments. Although the traditional APF algorithm can handle basic obstacle avoidance, its performance is limited under more demanding scenarios. The A* algorithm excels at generating the shortest paths with direct and precise trajectories, but its lack of smoothness can hinder motion efficiency in real-world applications. Meanwhile, the PRM algorithm demonstrates high adaptability and is particularly suitable for large-scale environments, yet its path quality is highly dependent on sampling density, often leading to unnecessarily lengthy routes. In summary, the

improved APF algorithm offers a balanced and robust solution, outperforming the other three algorithms and making it particularly effective for path planning in complex multi-AGV systems.

4. CONCLUSION

Multi-AGV path planning is a crucial technology in the automation of port terminal operations. By enabling precise route planning and real-time dynamic adjustments, this technology significantly reduces the risk of collisions and path conflicts among AGVs, thereby boosting both the efficiency and safety of port activities. It not only optimizes AGV travel routes and minimizes transportation time but also adeptly manages unexpected scenarios in complex port environments, ensuring that each AGV successfully completes its transportation tasks. This capability lays a strong foundation for the broader intelligent and automated development of port operations. We have developed an enhanced APF modeling framework designed to generate travel paths for AGVs. This framework is highly adaptable to various environmental conditions and is capable of providing safe and smooth transportation routes. The framework consists of four main steps: defining AGV transportation tasks, applying the improved APF algorithm to create potential forces for both target points and obstacles, calculating the repulsive forces between AGVs, and performing dynamic path planning and optimization. Initially, transportation tasks are assigned sequentially, with the AGV having the shortest transport distance selected for executing the next task, creating a prioritized list of transport tasks for each AGV in the port environment. In the next step, the initial state of each AGV - including position, speed, and direction - and transportation target points and obstacle data are initialized as inputs for the APF. The third step involves calculating the distances and repulsive forces between each AGV and others in the system. Steps two and three are repeated continuously until all AGVs successfully reach their respective target points.

While the improved APF algorithm shows strong performance in path planning and obstacle avoidance, there are still several areas that need further refinement for real-world port applications. First, the current scenario considers dynamic obstacles limited to AGVs, but ports also feature other moving elements such as vehicles and machinery. Effectively avoiding collisions and adjusting paths in such highly dynamic environments presents a significant challenge for the APF algorithm. Additionally, when AGVs are densely packed or operating simultaneously, the interaction of their potential fields can cause interference, leading to frequent path corrections and avoidance actions, which decreases overall operational efficiency. Moreover, the APF algorithm has limitations when handling complex terrains and non-convex obstacles, where AGVs may become trapped in local minima or deadlocks, preventing them from identifying globally optimal paths. Therefore, combining the APF algorithm with global path planning techniques and local optimization strategies will be essential for enhancing its effectiveness in the face of the complex, unpredictable conditions found in port environments.

The improved APF algorithm holds significant potential in future scientific and technological advancements. With the rapid development of artificial intelligence, the Internet of Things (IoT), and autonomous driving technologies, automated systems are increasingly applied in logistics, transportation, and manufacturing. The improved APF algorithm demonstrates notable advantages in multi-AGV systems, autonomous vehicle scheduling, and robotic navigation in complex environments, thanks to its efficient path planning, effective conflict avoidance, and smooth trajectory design. These strengths not only enhance system efficiency and reduce energy consumption and operational costs but also provide robust support for intelligent decision-making in dynamic and high-density environments. The improved APF algorithm can be further enhanced by integrating advanced technologies such as reinforcement learning, edge computing, and digital twins, allowing it to better adapt to and optimize dynamic, complex scenarios. For instance, incorporating deep learning could allow the algorithm to learn and respond to environmental changes in

real-time, making it more effective in handling unstructured and unpredictable settings. As quantum computing and distributed computing become more prevalent, the improved APF algorithm is expected to gain superior real-time processing capabilities and excel in large-scale multi-agent collaborative planning. Its potential applications extend across various fields, including traffic management in smart cities, optimized path planning for disaster relief robots, and autonomous navigation for space exploration missions. By addressing critical challenges in these domains, the improved APF algorithm stands to play a pivotal role in the development of next-generation intelligent systems, paving the way for safer, more efficient, and highly adaptive technologies in the future.

The improved APF algorithm demonstrates a clear advantage, producing shorter total transportation paths in multi-AGV parallel transport tasks. It outperforms the comparison algorithm in terms of both path safety and smoothness, contributing to improved port operation efficiency and a reduction in the likelihood of hazardous incidents.

DECLARATIONS

Authors' contributions

Writing - review and editing, supervision, formal analysis, conceptualization: Chen, X.

Writing - original draft, visualization, validation, methodology, investigation: Chen, C.

Formal analysis, conceptualization: Wu, H.

Writing - review, datacuration, conceptualization: Postolache, O.

Writing - review and editing, supervision, methodology, conceptualization: Wu, Y.

Availability of data and materials

The data that support the findings of this study are available from the corresponding author upon reasonable request.

Financial support and sponsorship

This work was jointly supported by the National Natural Science Foundation of China (Nos. 52331012, 52102397, 52472347), Open Fund of Chongqing Key Laboratory of Green Logistics Intelligent Technology (Chongqing Jiaotong University) (No. KLGLIT2024ZD001), and Open Fund of Jiangxi Key Laboratory of Intelligent Robot (No. JXINTROB-2024-201).

Conflicts of interest

Chen, X. is a Junior Editorial Board Member of the journal *Intelligence & Robotics* and Guest Editor of Special Issue “Intelligent, Safe, and Green Shipping-oriented Maritime Data Exploitation and Knowledge Discovery”. Chen, X. was not involved in any steps of editorial processing, notably including reviewers’ selection, manuscript handling and decision making. Wu, Y. is affiliated to the Qingdao Port Group Co., there is no potential conflict of interest between the authors and the company. The other authors declare that there are no conflicts of interest.

Ethical approval and consent to participate

Not applicable.

Consent for publication

Not applicable.

Copyright

© The Author(s) 2025.

REFERENCES

- Chen, J.; Ye, J.; Zhuang, C.; Qin, Q.; Shu, Y. Liner shipping alliance management: overview and future research directions. *Ocean. Coast. Manag.* **2022**, *219*, 106039. [DOI](#)
- Chen, J.; Zhuang, C.; Xu, H.; Xu, L.; Ye, S.; Rangel-Buitrago, N. Collaborative management evaluation of container shipping alliance in maritime logistics industry: CKYHE case analysis. *Ocean. Coast. Manag.* **2022**, *225*, 106176. [DOI](#)
- Han, Z.; Wang, D.; Liu, F.; Zhao, Z. Multi-AGV path planning with double-path constraints by using an improved genetic algorithm. *PLoS. One.* **2017**, *12*, e0181747. [DOI](#) [PubMed](#) [PMC](#)
- Sun, P. Z.; You, J.; Qiu, S.; et al. AGV-based vehicle transportation in automated container terminals: a survey. *IEEE. Trans. Intell. Transport. Syst.* **2023**, *24*, 341-56. [DOI](#)
- Miyombo, M. E.; Liu, Y.; Mulenga, C. M.; et al. Optimal path planning in a real-world radioactive environment: a comparative study of A-star and Dijkstra algorithms. *Nucl. Eng. Des.* **2024**, *420*, 113039. [DOI](#)
- Chen, X.; Liu, S.; Zhao, J.; Wu, H.; Xian, J.; Montewka, J. Autonomous port management based AGV path planning and optimization via an ensemble reinforcement learning framework. *Ocean. Coast. Manag.* **2024**, *251*, 107087. [DOI](#)
- Zhai, S.; Pei, Y. The dynamic path planning of autonomous vehicles on icy and snowy roads based on an improved artificial potential field. *Sustainability* **2023**, *15*, 15377. [DOI](#)
- Tang, G.; Tang, C.; Claramunt, C.; Hu, X.; Zhou, P. Geometric A-star algorithm: an improved A-star algorithm for AGV path planning in a port environment. *IEEE. Access.* **2021**, *9*, 59196-210. [DOI](#)
- Yin, X.; Cai, P.; Zhao, K.; Zhang, Y.; Zhou, Q.; Yao, D. Dynamic path planning of AGV based on kinematical constraint A* algorithm and following DWA fusion algorithms. *Sensors* **2023**, *23*, 4102. [DOI](#) [PubMed](#) [PMC](#)
- Meng, X.; Tang, J.; Yang, F.; Wang, Z. Lane-changing trajectory prediction based on multi-task learning. *Transp. Saf. Environ.* **2023**, *5*, tdac073. [DOI](#)
- Wu, B.; Zhang, W.; Chi, X.; Jiang, D.; Yi, Y.; Lu, Y. A novel AGV path planning approach for narrow channels based on the Bi-RRT algorithm with a failure rate threshold. *Sensors* **2023**, *23*, 7547. [DOI](#) [PubMed](#) [PMC](#)
- Li, Y.; Li, J.; Zhou, W.; Yao, Q.; Nie, J.; Qi, X. Robot path planning navigation for dense planting red jujube orchards based on the joint improved A* and DWA algorithms under laser SLAM. *Agriculture* **2022**, *12*, 1445. [DOI](#)
- Cui, G.; Yin, Y.; Xu, Q.; Song, C.; Li, G.; Li, S. Efficient path planning for automated valet parking: integrating hybrid A* search with geometric curves. *Int J Automot Technol* **2024**. [DOI](#)
- Sun, B.; Niu, N. Multi-AUVs cooperative path planning in 3D underwater terrain and vortex environments based on improved multi-objective particle swarm optimization algorithm. *Ocean. Eng.* **2024**, *311*, 118944. [DOI](#)
- Huang, T.; Fan, K.; Sun, W. Density gradient-RRT: An improved rapidly exploring random tree algorithm for UAV path planning. *Expert. Syst. Appl.* **2024**, *252*, 124121. [DOI](#)
- Wang, H.; Lai, H.; Du, H.; Gao, G. IBPF-RRT*: an improved path planning algorithm with Ultra-low number of iterations and stabilized optimal path quality. *J. King. Saud. Univ. Comput. Inf. Sci.* **2024**, *36*, 102146. [DOI](#)
- Xu, W.; Wang, Q.; Yu, M.; Zhao, D. Path planning for multi-AGV systems based on two-stage scheduling. *Int. J. Performability. Eng.* **2017**, *13*, 1347-57. [DOI](#)
- Huang, H.; Fang, Z.; Wang, Y.; Tang, J.; Fu, X. Analysing taxi customer-search behaviour using Copula-based joint model. *Transp. Saf. Environ.* **2022**, *4*, tdab033. [DOI](#)
- Zhou, Z.; Xu, L.; Qin, H.; Zhang, B.; Shang, G.; Xu, Z. A multi-AGV fast path planning method based on improved CBS algorithm in workshops. *Proc. Inst. Mech. Eng. C.* **2024**, *238*, 1507-21. [DOI](#)
- Wu, Z.; Su, W.; Li, J. Multi-robot path planning based on improved artificial potential field and B-spline curve optimization. In: 2019 Chinese Control Conference (CCC); 2019 Jul 27-30; Guangzhou, China. IEEE; 2019. pp. 4691-6. [DOI](#)
- Nazarahari, M.; Khanmirza, E.; Doostie, S. Multi-objective multi-robot path planning in continuous environment using an enhanced genetic algorithm. *Expert. Syst. Appl.* **2019**, *115*, 106-20. [DOI](#)
- Ning, Y.; Li, T.; Yao, C.; Du, W.; Zhang, Y. HMS-RRT: a novel hybrid multi-strategy rapidly-exploring random tree algorithm for multi-robot collaborative exploration in unknown environments. *Expert. Syst. Appl.* **2024**, *247*, 123238. [DOI](#)
- Liu, X.; Tang, J.; Yuan, C.; Gao, F.; Ding, X. Examining the characteristics between time and distance gaps of secondary crashes. *Transp. Saf. Environ.* **2023**, *6*, tdad014. [DOI](#)
- Mai, X.; Dong, N.; Liu, S.; Chen, H. UAV path planning based on a dual-strategy ant colony optimization algorithm. *Intell. Robot.* **2023**, *3*, 666-83. [DOI](#)
- Khatib, O. Real-time obstacle avoidance for manipulators and mobile robots. *Int. J. Robot. Res.* **1986**, *5*, 90-8. [DOI](#)